CrystEngComm

Accepted Manuscript

ROYAL SOCIETY OF CHEMISTRY

www.rsc.org/crystengcomm

CrystEngComm

COMMUNICATION

Cu^{II}-based metal-organic nanoballs for very rapid adsorption of dyes and iodine

Received 00th January 20xx,
Accepted 00th January 20xx

DOI: 10.1039/x0xx00000x

www.rsc.org/

Eder Amayuelas,[a] Arkaitz Fidalgo-Marijuán,[a] Begoña Bazán,*[,a,b] Miren-Karmele Urtiaga,[a] Gotzone Barandika,[c] and María-Isabel Arriortua[a,b]

Cu^{II}-nanoballs have been determined to be among the best MOPs (Metal-Organic Polyhedra) reported so far for the adsorption of small molecules, with the highlighting advantage of the rapid kinetics, which focuses applicability to the removal of emergent pollutants.

Organic dyes are nowadays widely used in many industries including medicine, textile, leather, printing and plastic.[1] The consequence of this fact is that dyes are present as emergent pollutants in soils and water where remain for large periods of time due to their high stability,[2] with potential risk of toxicity in wildlife and in humans.[3] On the other hand, the presence of iodine in soils, water and gas as nuclear activity pollutant product[4] or due to its extended use as germicide,[5] is still being a problem in many countries, which remembers the imperative need of its removal. Accordingly, several attempts to remove pollutants are being studied, such as the use of activated carbon,[6a] coagulation,[6b] photocatalysis[6c] or adsorption.[6d] This last method rose as one of the most feasible methods thanks to its efficiency and economic competitiveness.[7]

In this area, Metal-Organic Frameworks (MOF) have attracted great interest in recent years, taking a leading role in the field of catalysis,[8a] drug delivery,[8b] sensors[8c] and absorption.[8d] In the last decade, promising results have been reported specifically in the field of adsorption, based in the topology and chemical features of this type of porous materials.[9] Those are formed binding metal nodes with organic linkers generating porous networks, where the guest molecules accommodate when adsorption takes place. Many times these pores are originally occupied by solvent molecules that must be displaced, for efficient adsorption. Thus, it is common the activation of MOF with temperature to obtain an adsorbent material.[10] Therefore, an accurate characterization of the original compound as well as the activated one ensures greater efficiency of the adsorption process. In this context, this work presents the characterization of the activated compound **αMOP@Ei2-1** obtained from the already reported[11] $[Cu_{24}(m\text{-}BDC)_{24}(DMF)_{20}(H_2O)_4]\cdot 24DMF\cdot 40H_2O$ (**MOP@Ei2-1**), where *m*-BDC is 1,3-benzenedicarboxylic ligand and DMF is *N,N´*-dimethylformamide, as well as an study of dyes and iodine adsorption as pollutant examples, focusing on the kinetics of the rapid process.

Compound **MOP@Ei2-1** consists of a MOP formed by 24 Cu^{II} atoms grouped in 12 paddle-wheels linked by *m*-BDC. This arrangement generates a cuboctahedron structure with a large cavity within (1.6 nm of diameter), where crystallization and coordination H_2O and DMF molecules occupied the internal cavity, as well as the interstitial voids (Fig. 1). These structural units are nanoballs with a diameter of 2.4 nm. These nanoballs show two types of crevices: 8 triangular-like and 6 square-like ones (Fig. 1).

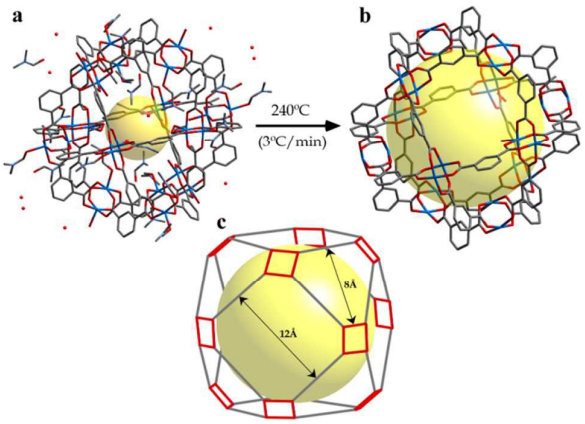

Fig 1. (a) View of the original **MOP@Ei2-1** (coordination and crystallization solvent molecules can be seen), (b) activated **αMOP@Ei2-1** and (c) geometry and dimensions of the two types of crevices.

[a] *Departamento de Mineralogía y Petrología, Universidad del País Vasco (UPV/EHU), Barrio Sarriena s/n, 48940 Leioa, Bizkaia*
[b] *BCMaterials, Basque Center for Materials, Applications and Nanostructures, Parque Tecnológico de Zamudio, Ibaizabal Bidea, Edificio 500-Planta 1, 48160 Derio, Bizkaia.*
[c] *Departamento de Química Inorgánica Universidad del País Vasco (UPV/EHU), Barrio Sarriena s/n, 48940 Leioa, Bizkaia.*
Electronic Supplementary Information (ESI) available: [Thermodiffactometry, Thermogravymetry, UV-Vis, FTIR]. See DOI: 10.1039/x0xx00000x

Thermal characterization of **MOP@Ei2-1** was reported previously.[11] The powdered compound maintains crystallinity up to 165 °C. However, nanoballs remain stable up to 280 °C (Fig. S1, ESI), when the CuO[12] residue begins to form. The amorphous phase occurs in the temperature range in which the *m*-BDC organic ligand still has not been degraded, according to thermogravimetry.[11] Having taking into account the latter, **αMOP@Ei2-1** was produced by heating **MOP@Ei2-1** at 240 °C during 1h (heating rate was 3 °C/min). This way, the adsorption capacity of the network was expected to be optimized.

In order to properly characterize the thermally activated **αMOP@Ei2-1**, IR spectroscopy and UV-Vis analyses were carried out. IR spectra of **MOP@Ei2-1** and **αMOP@Ei2-1** (Fig. S2, ESI) are similar. This fact means that there are no significant structural changes except for two bands: 1627 cm^{-1} and 3390 cm^{-1}. The intense band at 1627 cm^{-1}, which turns wider for the activated compound, corresponds to the elongation of C-N distances (related to coordinated DMF molecules). Changes in the band at 3390 cm^{-1} correspond to the disappearance of H-bonds. Diffuse reflectance UV-Vis measurements (Fig. S3, ESI) show similar spectra for the original and the activated samples, except for the loss of intensity in the band at 1913 nm which is related to the loss of coordination and crystallization water molecules inside and outside cuboctahedra. Therefore, the latter characterization confirms, as expected, that nanoballs keep integrity. Taking into account these facts, **αMOP@Ei2-1** was activated at 240 °C by removing solvent molecules. Obviously, at 240 °C, loss of the long-range organization is expected to take place. On the other hand, the absence of H_2O and DMF molecules in the network means that the accessible volume in the internal cavity of the nanoballs increases from 0.90 nm^3 to 2.14 nm^3 (Fig. 1). As a result, the porous **αMOP@Ei2-1** can exhibit adequate room to accommodate guest molecules.

Adsorption experiments were performed in aqueous and ethanol solution, after testing the stability of **MOP@Ei2-1** in these solvents (Fig. S4, ESI). Several dyes were tested as adsorbates: cationic methylene blue (**MB**) and rhodamine 6G (**R6G**), anionic methyl orange (**MO**) and congo red (**CR**), and neutral dimethyl yellow (**DY**) (Fig S5, ESI). Besides, iodine ($\mathbf{I_2}$) was also tested.

Typically, 10 mg of **αMOP@Ei2-1** was added into 4 mL glass beaker containing 1 x 10^{-4} mol·L^{-1} of **MB**, **RB**, **MO**, or **CR** aqueous solution and **DY** and $\mathbf{I_2}$ ethanol solution. After 7 days, the colors of the solutions became pale (Fig. 2), indicating the adsorption process having been occurred.

The adsorption of dyes was confirmed by IR spectroscopy for **MB**, **CR** and **DY** (Fig. S6, ESI). For samples of **αMOP@Ei2-1** loaded with **MB**, **CR** and **DY** a band at 1690 cm^{-1} can be observed, which can be assigned to C-N bonds. Additionally, for **αMOP@Ei2-1** samples loaded with **CR** and **MB**, two bands are observed at 1310 and 3590 cm^{-1} associated with C-S and N-H bonds, respectively. The observance of these bands in the IR spectra confirms the successful immobilization of **MB**, **CR** and **DY** molecules into **αMOP@Ei2-1** nanoballs.

In order to quantify the process, previous calibration was carried out by means of UV-Vis absorption at selected wavelengths.

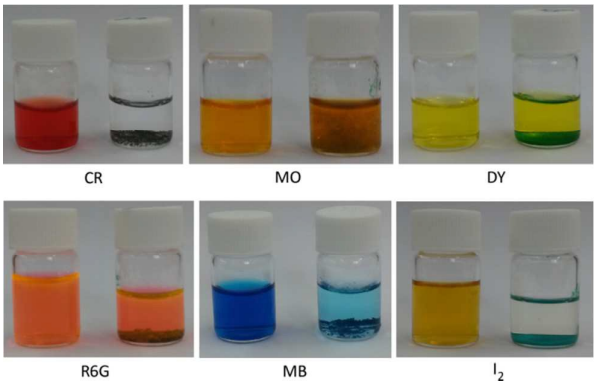

Fig. 2 Color changes of dyes and iodine solutions. All photos were taken after 7 days since the addition of **αMOP@Ei2-1**.

This way, samples of the dissolution to be monitored were taken while adsorption process was occurring and the results can be seen in Fig. S7-S12, ESI.

The removed quantity of dyes adsorbed at equilibrium by **αMOP@Ei2-1** expressed in mmol per gram of **αMOP@Ei2-1** was calculated by the following equation.[13]

$$Qeq = \frac{C0 - Ceq}{m} V \qquad (1)$$

where Q_{eq} (mmol g^{-1}) is the amount of adsorbed dyes by **αMOP@Ei2-1**, C_0 (mmol L^{-1}) is the initial concentration of dyes in the water, C_{eq} (mmol L^{-1}) is the equilibrium concentration of dyes remaining in the water, V (L) is the volume of the aqueous solution, and m (g) is the weight of used **αMOP@Ei2-1**.

As represented in the adsorption histogram (Fig. S13, ESI), 1 g of **αMOP@Ei2-1** can adsorb 0.0356 mmol of **MB**, 0.012 of **DY**, 0.14 mmol of $\mathbf{I_2}$ and 0.0395 mmol of **CR** As consequence, after the adsorption tests, the color of the resulting solid powder sample transforms into dark blue (**MB**), light green (**DY** and $\mathbf{I_2}$) and dark brown (**CR**) (Fig. S14, ESI).

Previous results indicate that in the case of $\mathbf{I_2}$, there is an absorption of 0.77 molecules per nanoball. Values for dyes are also outstanding: 0.20, 0.22 and 0.07 molecules or ions per nanoball for **MB**, **CR** and **DY**, respectively.

In order to study the kinetics of adsorption, the *in situ* UV/Vis absorption was measured in the dark at room temperature[14] during 7600 min for **CR**, **DY**, and $\mathbf{I_2}$, and during 240 min for **MB**. Thus, 10 mg of **αMOP@Ei2-1** was soaked in a Quartz SUPRASIL® cell with 4 mL of dye-contaminated water (1 x 10^{-4} mol·L^{-1}) for **MB** and **CR** and ethanol (1 x10^{-4} mol·L^{-1}) for **DY** and $\mathbf{I_2}$ (1 x 10^{-3} mol·L^{-1}). Figure 3 shows the kinetic of the adsorption processes. As observed, adsorption takes place in two steps. The first one is very rapid, while the second one is much slower. The adsorption is especially rapid for **MB**, $\mathbf{I_2}$ and **CR**. It is noteworthy that 96.6 % of **MB** is adsorbed in 15 minutes while other authors report that several hours are required to adsorb a similar quantity of the same dye.[15]

Adsorption kinetics was adjusted to a first order, with the aim of comparing our results with previous ones.

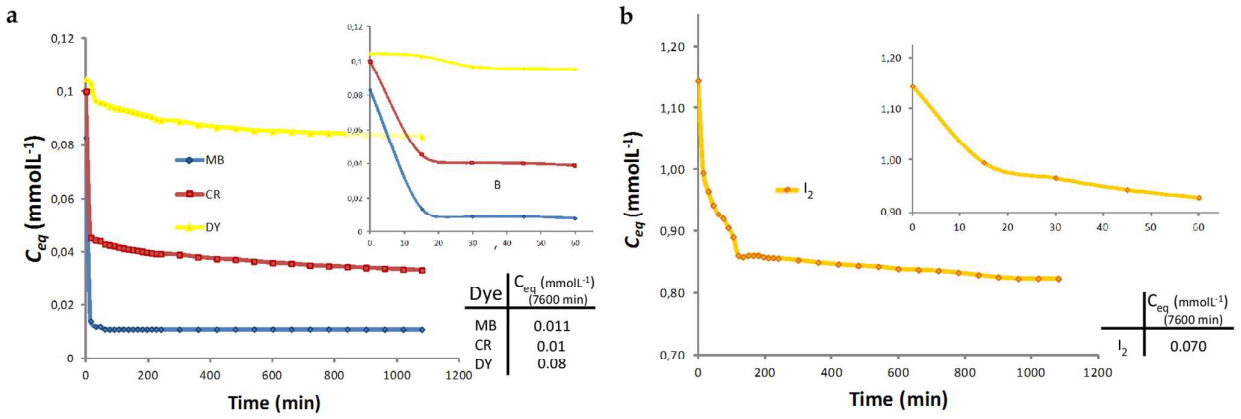

Fig. 3 Concentration changes for (a) **MB** (blue), **CR** (red), **DY** (yellow), and for (b) I_2 (orange). All dyes and iodine remains stable except for **CR**, which continues adsorbing.

Due to the presence of two kinetic steps, adsorption rate constants were calculated for the first one where most of the adsorption has taken place. Thus, calculated adsorption rate constants for **MB**, **CR,** I_2 and **DY** are 4.8 x 10^{-2}, 2.1 x 10^{-2}, 1.2 x 10^{-3} and 2 x 10^{-3} min^{-1}, respectively (Fig. S15, ESI).

It is worth mentioning that the sizes of **MB**, **CR** and **DY** are in the range of the dimensions for the square crevices (Fig. 1). However, the different kinetics of dye adsorptions can be attributed to the synergy among the dimensions, shapes (Table S1, ESI) and ionic strength.[16] Thus, although the size of **CR** is larger than **DY**, the ionic strength of **CR** solution is higher than **DY**. Therefore, absorption kinetics of **CR** is more rapid than **DY**. On the other hand, **MB** is smaller than **CR,** and this makes possible its faster adsorption.

Comparison of the results herein presented with others reported elsewhere[17] indicates that **αMOP@Ei2-1** is among the best of the adsorption MOPs. Moreover, the adsorption velocity is remarkable for three of the four studied adsorbates. In fact, just the compound reported by Zhu *et. al.*[17b] is clearly superior to **αMOP@Ei2-1**.

Dye release experiments were also carried out soaking dye charged samples into NaCl aqueous solution. After 24 h the adsorbent was removed from the solution and the concentration of the liquid was measured by UV-Vis. The results indicate that the desorbed amount for MB is significantly high (2.6 x10^{-3} mmol·L^{-1}, 30% of the adsorbed dye). For the other dyes desorption rates are much lower: CR: 1.43x10^{-5} mmol·L^{-1} (0.1%), DY: 4.05x10^{-3} mmol·L^{-1} (5%), and iodine: 1.94x10^{-2} mmol·L^{-1} (2.5%).

In summary, a good thermal and structural characterization of the original **MOP@Ei2-1** has been required to design an appropriate thermal activation focused to optimize the adsorption capacity while keeping integrity of the nanoballs in **αMOP@Ei2-1**. Preliminary investigations for **αMOP@Ei2-1** indicate that adsorption is size-dependent which can be used for the removal of emergent pollutants from natural waters. Rapidness in adsorption is the most relevant feature of **αMOP@Ei2-1.**

This work has been financially supported by the ''Ministerio de Economia y Competitividad'' (MAT2013-42092-R), the ''Gobierno Vasco'' (Basque University System Research Groups, IT-630-13) and UPV/EHU (UFI11/15) which is gratefully acknowledge. The authors acknowledge the support received by the European Regional Development Fund (ERDF). The technical and human support provided by SGIker (UPV/EHU) is gratefully acknowledged. Eder Amayuelas thanks the University of the Basque Country UPV/EHU for his formation scholarship.

Notes and references

1 G. Crini, *Bioresour. Technol.*, 2006, **97**, 1061.
2 *(a)* C. Zou, Z. J. Zhang, X. Xu, Q.H. Gong, J. Li and C. D.Wu, *J. Am. Chem. Soc.*, 2012, **134**, 87; *(b)* M. A. Al-Ghouti, M. Khraisheh, S. J. Allen and M. N. Ahmad, *J. Environ. Manage.*, 2003, **69**, 229; *(c)* L. Zhou, C. Gao and W. Xu, *ACS Appl. Mater. Interfaces*, 2010, **2**, 1483.
3 *(a)* M. A. Al-Ghouti, M. Khraisheh, S. J. Allen and M. N. Ahmad, *J. Environ. Manage.*, 2003, **69**, 229; *(b)* M. T. Uddin, M. A. Islam, S. Mahmud and M. Rukanuzzaman, *J. Hazard. Mater.*, 2009, **164**, 53.
4 N. Mnasri, C. Charnaya, L. C. Ménorval, Y. Moussaoui, E. Elaloui and J. Zajac, *Micropor. Mesopor. Mat.,* 2014, **196**, 305.
5 R. L. Boddie and S. C. Nickerson, *J Dairy Sci*, 1997, **80**, 1846.
6 *(a)* J. W. Lee, S. P. Choi, R. Thiruvenkatachari, W. G. Shim and H. Moon, *Water Res.*, 2006, **40**, 435; *(b)* B. Y. Shi, G. H. Li, D. S. Wang, C. H. Feng and H. X. Tang, *J. Hazard. Mater.*, 2007, **143**, 567; *(c)* J. Fernández, J. Kiwi, C. Lizama, J. Freer, J. Baeza and H. D. Mansilla, *J. Photochem. Photobiol. A*, 2002, **151**, 213; *(d)* D. Mahanta, G. Madras, S. Radhakrishnan and S. Patil, *J. Phys. Chem. B*, 2008, **112**, 10153.
7 *(a)* Q. R. Fang, G. S. Zhu, Z. Jin, Y. Y. Ji, J. W. Ye, M. Xue, H. Yang, Y.Wang and S. L. Qiu, *Angew. Chem., Int. Ed.*, 2007, **46**, 6638; *(b)* A. Afkhami and R. Moosavi, *J. Hazard. Mater.*, 2010, **174**, 398; *(c)* H. Y. Zhu, R. Jiang and L. Xiao, *Appl. Clay Sci.*, 2010, **48**, 522; *(d)* S. Qadri, A. Ganoe and Y. Haik, *J. Hazard. Mater.*, 2009, **169**, 318; *(e)* A. Afkhami, T. Madrakian and A. Amini, *Desalination*, 2009, **243**, 258; *(f)* A. Afkhami, T. Madrakian, A. Amini and Z. Karimi, *J. Hazard. Mater.*, 2008, **150**, 408.
8 *(a)* J.Y. Lee, O.K. Farha, J. Roberts, K.A. Scheidt, S.T. Nguyen and J.T. Hupp, *Chem. Soc. Rev.*, 2009, **38**, 1450; (b) H. Deng, S. Grunder, K. E. Cordova, C. Valente, H. Furukawa, M. Hmadeh, F. Gándara, A. C. Whalley, Z.

Liu, S. Asahina, H. Kazumori, M. O'Keeffe, O. Terasaki, J. F. Stoddart and O. M. Yaghi, *Science*, 2012, **336**, 1018. *(c)* R.J. Kuppler, D.J. Timmons, Q.-R. Fanga, J.-R. Li, T.A. Makal, M.D. Young, D. Yuan, D. Zhao, W. Zhuang and H.-C. Zhou, *Coord. Chem. Rev.,* 2009, **253**, 3042; *(d)* J.-R. Li, J. Yu, W. Lu, L.-B. Sun, J. Sculley, P.B. Balbuena and H.-C. Zhou, *Nat. Commun.*, 2013, **4**, 1538;

9 *(a)* Y. C. He, J. Yang, Y.-Y. Liu and J.-F. Ma, *Inorg. Chem*., 2014, **53**, 7527; *(b)* R. Custelcean, *Chem. Soc. Rev.*, 2014, **43**, 1813; *(c)* M. Zhao, S. Ou and C.-D. Wu, *Acc. Chem. Res.*, 2014, **47**, 1199; *(d)* M. O'Keeffe and O. M. Yaghi, *Chem. Rev.*, 2012, **112**, 675;

10 *(a)* K. Peikert, L. J. McCormick, D. Cattaneo, M. J. Duncan, F. Hoffmann, A. H. Khan, M. Bertmer, R. E. Morris and M. Froba, *Micropor. Mesopor. Mat.*, 2015, **216**, 118; *(b)* Z. H. Rada, H. R. Abid, H. Sun and S. Wang, *J. Chem. Eng. Data*, 2015, **60**, 2152; *(c)* A. Schneemann, S. Henke, I. Schwedler and R. A. Fischer, *ChemPhysChem*, 2014, **15**, 823.

11 E. Amayuelas, A. Fidalgo-Marijuan, G. Barandika, B. Bazán, M. K. Urtiaga and M. I. Arriortua, *CrystEngComm*, 2015, **17**, 3297.

12 S. Asbrink and L. J. Norrby, *Acta Crystallogr., Sect. B: Struct. Sci., Cryst. Eng. Mater.*, 1970, **26**, 8.

13 G. Crini, *Dyes Pigm.*, 2008, **77**, 415.

14 Y. C. He, J. Yang, G. C. Yang, W. Q. Kan and J. F. Ma, *Chem. Commun.*, 2012, **48**, 7859.

15 *(a)* X. X. Huang, L. G. Qiu, W. Zhang, Y. P. Yuan, X. Jlang, A. J. Xie, Y. H. Shen and J. F. Zhu, *CrystEngComm*, 2012, **14**, 1613; *(b)* C. Mondal, M. Ganguly, J. Pal, R. Sahoo, A. K. Sinha and T. Pal, *Chem. Commun.*, 2013, **49**, 9428.

16 *(a)* M. B. Dewal, M. W. Lufaso, A. D. Hughes, S. A. Samuel, P. Pellechia and L. S. Shimizu, *Chem. Mater.*, 2006, **18**, 4855; *(b)* Q. K. Liu, J. P. Ma and Y. B. Dong, *Chem. Commun.*, 2011, **47**, 12343.

17 *(a)* Y. C. He, J. Yang, W. Q. Kan and J. F. Ma, *CrystEngComm*, 2013, **15**, 848; *(b)* Z. Zhu, Y. L. Bai, L. Zhang, D. Sun, J. Fanga and S. Zhu, *Chem. Commun.*, 2014, **50**, 14674; *(c)* Y. C. He, J. Yang, W. Q. Kan, H. M. Zhang, Y. Y. Liu and J. F. Ma, *J. Mater. Chem. A*, 2015, **3**, 1675; *(d)* X. L. Lv, M.Tong, H. Huang, B. Wang, L. Gan, Q. Yang, C. Zhong and J. R. Li, *J. Solid State Chem.*, 2015, **223**, 104.

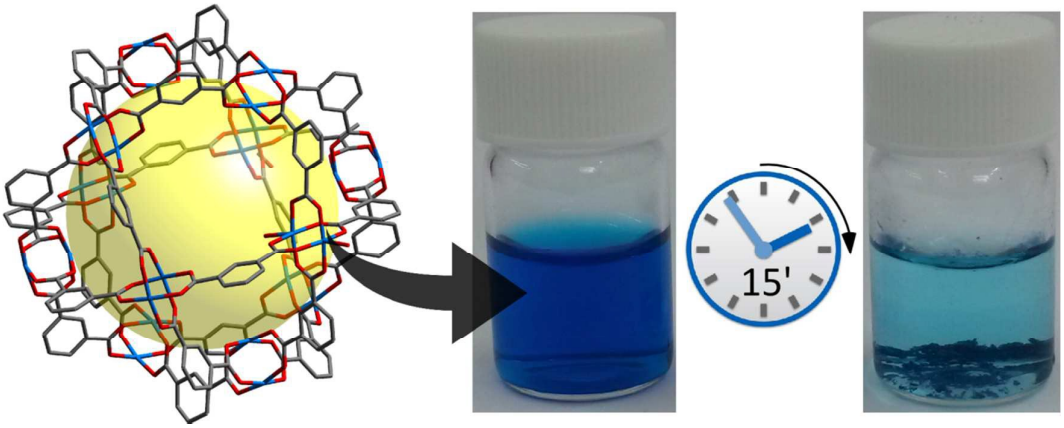

MOP nanoballs for rapid adsorption of dyes and iodine